Role of Ionic Strength on Hemoglobin Interparticle Interactions and Subunit Dissociation from Light Scattering

Sabrina Beretta, Giuseppe Chirico, Daniele Arosio, and Giancarlo Baldini*

Istituto Nazionale Fisica della Materia and Dipartimento di Fisica, Università degli Studi di Milano, Via Celoria 16, 20133 Milano, Italy

Received July 28, 1997; Revised Manuscript Received September 23, 1997[⊗]

ABSTRACT: The average diffusion coefficients of hemoglobin (bovine CO-Hb) in dilute solutions (ϕ = 0.005), as obtained by cumulant analysis of the autocorrelation functions of the scattered light, are found to depend upon pH and ionic strength. A decrease of the diffusion coefficient is observed vs ionic strength for two salts, NaCl or $CaCl_2$, in the range 10−300 mM, when the solution pH is away from that corresponding to the isolectric point of the protein. It is shown here that the results can be interpreted in terms of electrostatic effects with a model that should include both interparticle interactions and subunit dissociation of the protein. Global analyses of the first cumulant diffusion coefficient vs ionic strength were then applied in order to obtain accurate values of the hemoglobin charge vs pH and of its single particle diffusion coefficient. A quantitative estimate of the dissociation was also obtained, leading then to good descriptions both of the electrostatic and of the non-electrostatic contribution to the protein tetramer to dimer dissociation process.

1. Introduction

The aggregation or dissociation of proteins has important influence on their functions. Proteins in vivo are often found at concentrations large enough to give rise to substantial interactions that facilitate intermolecular and also intersubunit interactions and aggregation. These have been the subject of several investigations, and the study of them has become more and more valuable also in protein crystallization.[1] Two major unspecific factors affect protein interactions: the protein charge, mainly determined by pH, and the ionic strength, caused by the presence of small electrolytes in solution. Except for some specific salt−protein interactions, one of the major effects of electrolytes is the screening of protein−protein electrostatic interactions. In both precipitation and crystallization, electrostatic shielding of the protein charge is needed for their interactions. It is therefore interesting to study the change in aggregation/dissociation with ionic strength. Light scattering has been recognized as a powerful tool to study molecular weights (static light scattering) and diffusional properties (dynamic light scattering) due to the low perturbation on protein solution induced by light. The general theory and significant applications of dynamic light scattering to colloidal and protein solutions can be found in the literature on the subject.[2−6] In more recent studies,[7] light scattering has been used to characterize the nucleation conditions and protein aggregation by following the change of the diffusion coefficient with the mass of the aggregate. However, in order to fully exploit the information carried by light scattering, one should take into account the effect of protein−protein interaction not only on their aggregation/dissociation processes but also on the observed diffusion coefficient itself. It has been shown previously that, depending on the ionic strength and pH, intermolecular interactions can affect substantially the diffusion coefficient even at a rather low protein volume fraction.[8]

The aim of the present work has been the study of interparticle interactions and dissociation of bovine carboxyhemoglobin vs ionic strength for two salts, NaCl and $CaCl_2$, at different charges obtained by varying the solution pH. This has been performed by following the relaxation rate of the autocorrelation functions of the scattered light and by analyzing the data by models that take into account either the intermolecular interactions, or the aggregation or both. The use of a model that gives relevance to intermolecular interactions is expected to lead to a better description of the electrostatic and nonelectrostatic contribution to dissociation.

In this paper a theoretical introduction to the effects of interparticle interactions and dissociation on the first cumulant diffusion coefficient D_z is given in order to describe the model applied to the experimental data. Details on measurements and data fitting are given in the Experimental Section. In the Discussion the single sets of data corresponding to different pH values are separately fitted vs ionic strength I_s or fitted all together in a global analysis. Conclusions on the protein interactions and parameters are then drawn.

2. Theoretical Background

Hemoglobin is a tetrameric protein (molecular weight 64 500)[9] made of two pairs of α and β subunits ($\alpha^2\beta^2$) that can dissociate into dimers ($\alpha\beta$) depending on its global charge and ionic strength, and, under particular experimental conditions, into monomers.[10] In the following, only the tetramer to dimer equilibrium will be considered and described by a dissociation constant $\tilde{L}$

$$\tilde{L} = \exp(-\Delta G_{diss}/K_B T) \quad (1)$$

where ΔG_{diss} is the molecular dissociation free energy associated with the reaction. The constant $\tilde{L}$ can be written in terms of the corresponding molar concentrations of tetramers [T] and dimers [D] as: $\tilde{L} = [D]^2/[T]$ or, more conveniently redefined, in terms of the tetramer dissociated fraction x as

$$L_{diss} = \tilde{L} M_T = 4cx^2/(1 - x) \quad (2)$$

where M_T is the tetramer weight, c is the total weight concentration, and x is defined as

[⊗] Abstract published in *Advance ACS Abstracts,* November 1, 1997.

S0024-9297(97)01137-6 CCC: $14.00

$$x = \frac{c_D}{c_D + c_T}$$

with

$$c = c_D + c_T \tag{3}$$

Therefore, $c_D = x\,c$ and $c_T = (1 - x)c$. Then eq 2 can be solved with respect to the dissociated fraction x:

$$8cx = -L_{diss} + (L_{diss}{}^2 + 16L_{diss}c)^{1/2} \tag{4}$$

This equation can be useful for obtaining information on the chemical equilibrium, i.e. ΔG_{diss}, from light scattering measurements vs different solution parameters such as ionic strength, pH, or protein concentration.

The total free energy ΔG_{diss} is assumed to derive from the sum of two contributions:[11]

$$\Delta G_{diss} = \Delta G_{nel} + \Delta G_{el} \tag{5}$$

The nonelectrostatic free energy term, ΔG_{nel}, is the term remaining after considering the charging process of the protein in ionic solutions and which is responsible of the electrostatic free energy term, ΔG_{el}. As to the latter contribution, one can evaluate an enthalpic contribution ΔH_{el}, due to the electrostatic potential around the protein, and an entropic term, ΔS_{el}, due to the ordering process of the counterions around the macroion. It has been shown that the resulting free energy can also be calculated as[12]

$$\mu_{el} = \Delta H_{el} - T\Delta S_{el} = \int_0^Q \psi_a(q,r = a)\,dq \tag{6}$$

where $\psi_a(Q,r)$ is the electrostatic potential around a spherical macroion of radius a and charge Q embedded in an electrolyte solution. Within the approximations of the Debye−Hückel theory one can write[13]

$$\mu_{el} = \frac{Q^2e^2}{2\epsilon a}\left(1 - \frac{\kappa a}{1 + \kappa(a + s)}\right) \tag{7}$$

where e is the proton charge ($e = 4.81 \times 10^{-10}$ esu), ϵ is the solution dielectric constant, s is the radius of the counterions, and κ is the inverse Debye screening length

$$\kappa = \left(\frac{8\pi N_{AV}e^2}{1000\epsilon K_B T}\right)^{1/2} I_s{}^{1/2} \tag{8}$$

where I_s indicates the solution ionic strength in molar units. Finally from eq 7 one can define the electrostatic contribution to ΔG_{diss} as the difference in the electrostatic part of the chemical potential of tetramers $\mu_{T,el}$ and dimers $\mu_{D,el}$ according to

$$\Delta G_{el} = 2\mu_{D,el} - \mu_{T,el} \tag{9}$$

The electrostatic free energy term ΔG_{el} depends mainly upon the solution ionic strength I_s, the particle size a, and the charge Q.

The tetramer−dimer equilibrium of hemoglobin has been studied in previous works by photon correlation spectroscopy.[8,11,14] This technique measures the molecular diffusion coefficients from the relaxation decay of the autocorrelation function ACF of the light scattered by the solution. The measured ACF is assumed to be the sum of two exponential decays corresponding to the tetramer's and dimer's translational relaxation decays. In fact, tetramer-to-dimer kinetics[15] has a rate constant $\leq 10^2$ Hz, much smaller than the autocorrelation function relaxation rate, $\Gamma \simeq 10^4$ Hz. However the ratio of the dimer to tetramer translational diffusion coefficients, evaluated[14] to be $\Omega = 1.205$, is not sufficiently large to allow resolution of the individual relaxation components of the ACF by a nonlinear double-exponential fitting on experimental data always affected by the presence of some statistical noise. Then the ACF is found to be well represented by a single-exponential decay, and it can be characterized by the first two cumulant coefficients. As a matter of fact, the first cumulant diffusion coefficient is affected by the tetramer−dimer equilibrium and by the electrostatic interactions between proteins in solution, and it can be expressed,[16] according to a model recently suggested,[8] as

$$D_z = D_z{}^o(1 + \tilde{k}\phi) \tag{10}$$

where the volume fraction ϕ is related to the partial molecular volume $\bar{v}$ and the mass concentration c by $\phi = c\bar{v}$, which in the present experimental conditions of $c \simeq 5$ mg/mL is $\phi \simeq 0.005$. The average single particle diffusion coefficient D_z^o and the interaction constant $\tilde{k}$ are defined by[8]

$$D_z^o = \frac{2(1 - x)D_T^o + xD_D^o}{2 - x} = D_T^o\frac{2(1 - x) + x\Omega}{2 - x} \tag{11}$$

$$\tilde{k} = \frac{2(1 - x)^2k_{TT} + \Omega x^2k_{DD} + (2 + \Omega)x(1 - x)k_{TD}}{2(1 - x) + \Omega x} \tag{12}$$

where D_T^o and D_D^o are the tetramer and dimer single particle translational diffusion coefficients ($D_D^o = \Omega D_T^o$) and the tetramer dissociated fraction x is a function (see eq 4) of L_{dis} and protein concentration c. The interaction constants k_{TT}, k_{DD}, and k_{TD} between tetramers, dimers and between tetramers and dimers in eq 12 are evaluated according to a treatment of both direct and hydrodynamic interactions on the Brownian movement of the particles in solution[17]

$$k = k_0 + \int_{x_0}^{x_\infty} F(\rho)(e^{-W(\rho)/KT} - 1)\,d\rho \tag{13}$$

where $\rho = (r - 2a)/2a$ and the integral bounds are usually set to $x_0 \leq 0.06$ and $x_\infty = 20$ for numerical applications (see Experimental Section). The hydrodynamic function $F(\rho)$ has the functional form given by Felderhof,[17,18] as thoroughly discussed.[8] The electrostatic intermolecular energy $W_{EL} = W_{1,2}$ (i.e $W_{T,T}$, $W_{T,D}$, $W_{D,D}$) between charged spherical molecules can be well approximated[8] from a multipole expansion[19] as

$$W_{EL} = W_{1,2}(\rho) = \frac{Q_1Q^2e^2}{\epsilon(a_1 + a_2)(1 + \kappa_D a_1)(1 + \kappa_D a_2)}\frac{\exp(-\kappa_D(a_1 + a_2)\rho)}{(1 + \rho)} \tag{14}$$

where ρ has been defined as

$$\rho = \frac{r - (a_1 + a_2)}{(a_1 + a_2)} \tag{15}$$

and Q_1, Q_2 and a_1, a_2 are the charges and the radii of the two particles, tetramers and dimers, approximated to spheres. The tetramer's and dimer's radii and charges are assumed to be related as follows: $Q_D = Q_T/2$, and $a_D = a_T/\Omega$. At very short intermolecular distance a steep attractive potential due to Van der Waals interactions is needed as in the form[20]

$$W_{VW}(\rho) = -\frac{H}{12}\left[\frac{1}{(\rho+1)^2} + \frac{1}{\rho^2+2\rho} + 2\ln\left(\frac{\rho^2+2\rho}{(\rho+1)^2}\right)\right] \tag{16}$$

where H is the Hamaker constant. The total intermolecular energy is $W = W_{VW} + W_{EL}$. Since W_{VW} has a singularity at $\rho = 0$, an arbitrary lower cutoff $x_0 = 0.06$, imagined as due to the size of a salt ion in solution, 0.18 nm,[21] has been assumed in the integration of eq 13 similar to previous choices.[7,17]

3. Experimental Section

3.1. Bovine Carboxyhemoglobin. Bovine Carbonylhemoglobin (COHb) was kindly provided and purified by ionic exchange HPLC techniques[22] by Dr. E. Bucci (University of Maryland) and stored in liquid nitrogen at the concentration of ≃9% in weight and ionic strength of ≃55 mM. In order to perform the measurements at the desired protein concentration, (5 mg/mL), the sample stock was prepared by dilution of the freshly thawed stock with an appropriate amount of carbon monoxyde saturated buffer brought at the proper I_s (in the range $10 \le I_s \le 300$ mM) by addition of either NaCl or $CaCl_2$. All solutions were prefiltered with 0.22 μm Millipore filter. The COHb solutions have been titrated with *HCl* or *NaOH* (0.1 M) to adjust the proton concentration as desired. The pH determinations were made using a radiometer HI 8417−type pH meter and checked before and after scattering measurements. $CaCl_2$−hemoglobin solutions have been prepared at the following pH values: pH = 5.37 ± 0.17 in acetate (CH_3-COOH − NaOH) buffer, pH = 7.19 ± 0.1 in Tris (Tris − HCl), pH = 9.11 ± 0.12 and pH = 9.41 ± 0.13 in borate ($Na_2B_4O_7 \cdot 10H_2O$−NaOH) buffer. Phosphate (KH_2PO_4−Na_2HPO_4) and borate buffers have been employed with NaCl salt in order to prepare hemoglobin solution at pH = 7.31 ± 0.06 and pH = 9.27 ± 0.2, respectively, since precipitation of the phosphate buffer in the presence of $CaCl_2$ has been observed. In order to avoid the presence of Cl^- ions, hemoglobin solutions at different ionic strengths and pH = 9.5 ± 0.15 have been also obtained by varying the $Na_2B_4O_7$ concentration. In the computation of the total ionic strength of the solution, the contribution of the buffer, of the added electrolytes, and of the hemoglobin stock are taken into account under the assumption of additivity of the single ionic strength contribution. For most of the measured solutions, the dominant part is found to be that of the added salts.

The total COHb concentration and the presence of methemoglobin (MetHb) has been measured spectrophotometrically, before and just immediately after the PCS measurements, using the extinction coefficients of the COHb and MetHb species at the two wavelengths of 540 and 630 nm :[23] the presence of MetHb in solution has always been found to be less than a few percent. The hemoglobin sample, prefiltered with 0.22 μm Millipore filters, was gently injected in the scattering cell, previously carefully cleaned, through 0.1 μm Nucleopore polycarbonate filter. The sample cell and the filter were always equilibrated with the same buffer used to dilute the sample.

3.2. Measurement of Diffusion Coefficient *D*. The scattering cell, a cylindrical Hellma quartz cell, 8 mm internal diameter, was surrounded by a larger cylindrical cell with an index-matching liquid and the temperature kept at 25 ± 0.2 °C as checked with a thermocouple.

The optical source of the light scattering apparatus was a 632.8 nm He--Ne (25 mW) laser and the time-dependent correlation function of the scattered intensity was measured at a scattering angle $\theta = 60°$ and processed with a Brookhaven BI2030AT correlator using a sample time of 2 μs. Further details about the apparatus can be found elsewhere.[14]

The intensity autocorrelation function was fitted to a second-order cumulant[24] trial function, in order to obtain the diffusion coefficient D_z from the first cumulant $\bar{\Gamma}$ and to detect polydispersity of samples. Following the criteria discussed in a previous work,[25] at least eight autocorrelation functions have been collected, at all conditions studied here, each with a baseline $B \ge 250\,000$ counts and with polydispersity ≤0.05. The expected changes in polydispersity due to tetramer−dimer equilibrium or intermolecular interactions in Hemoglobin solutions fall within the statistical noise affecting the ACFs.

The first cumulant diffusion coefficient is reported to standard conditions of water at 20 °C and called hereafter $D_z^{[20]}$. Accurate determination of the diffusion coefficient D_z requires the value of the refraction index n_R and solution viscosity corrections mainly due to the added electrolytes.[26] At $c \simeq 5$ mg/mL, the correction to the solution refraction index n_R due to the finite hemoglobin concentration[27] was considered to be negligible. Moreover local heating effects, due mainly to the presence of some methemoglobin, have been subtracted by extrapolating the measured diffusion coefficient to zero laser power[28] for each sample. The estimated uncertainty on the measured diffusion coefficient due to the above corrections is ≃0.7%, being largely due to the strong temperature dependence of the viscosity.

3.3. Fitting Procedures. Data obtained by processing the measured ACF, i.e., the first cumulant diffusion coefficients $D_z^{[20]}$, were further fitted with a nonlinear least-squares methods to the theoretical function given in eq 10. The data sets, corresponding to different experimental conditions, i.e., different proton concentrations (pH) and ionic strengths I_s can be fitted separately (single set fit) or all together in a global analysis. The latter technique is well suited to establish relations that may exist between different conditions and it suggests physical models to describe the system under study. Both fitting procedures (i.e. single set fit and global analysis) were performed by means of the Levenberger−Marquardt algorithm.[29] This method combines a gradient search and a Taylor expansion of the fitting function into a single algorithm. The fitting programs, written in C language, made use of the Marquardt subroutines of the Numerical Recipes library (MRQMIN[30]) and ran on HP and or on SGI workstation. The theoretical model used in the fitting procedure (eq 10) needed the evaluation of an integral (see eq 13) which was performed by a standard routine (QTRAP[30]). Tests on the convergence of this routine were performed by studying the trend of the integral function vs the integral upper bound (x_∞; see eq 10) and finding changes less than 0.01% for $x_\infty \ge 20$. The fitting program requires some physical constraints, i.e., the positive Hamaker constant H and dissociation constant $L_{diss} = \exp(-\Delta G_{diss})$. This was performed by fitting the logarithm of the positive-constraint parameters.

4. Results

The autocorrelation functions (ACF) of the scattered light from hemoglobin solution were collected at protein concentration $c \simeq 5$ mg/mL and temperature $T \simeq 25$ °C vs ionic strength I_s in the range $10 \le I_s \le 300$ mM at different pH values (in acid, neutral and alkaline conditions). In order to obtain the desired ionic strength an appropriate amount of NaCl or $CaCl_2$ has been added to the Hemoglobin solutions.

The ACFs analysis with the cumulants method gives the value of the first cumulant diffusion with uncertainties evaluated on several (eight or more) independent measurements.

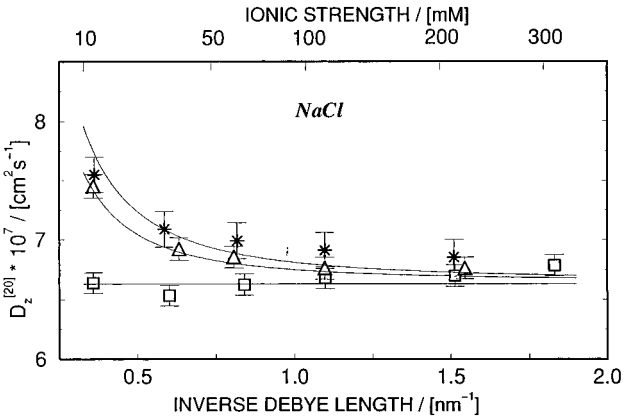

Figure 1. Experimental diffusion coefficient $D_z^{[20]}$ vs the inverse of Debye screening length (or ionic strength) measured at a hemoglobin concentration $c \simeq 5$ mg/mL. Varying ionic strengths ($10 \leq I_s \leq 300$ mM) are obtained by adding NaCl to the proper buffer at $I_s \simeq 10$ mM for pH = 5.0 (*), 7.3 (□), and 9.3 (△). The data at acid condition (pH = 5.0) are from Lunelli et al. (1994). Solid lines are the best fit with the global analysis described in the text ($H = 4.5$, Table 2).

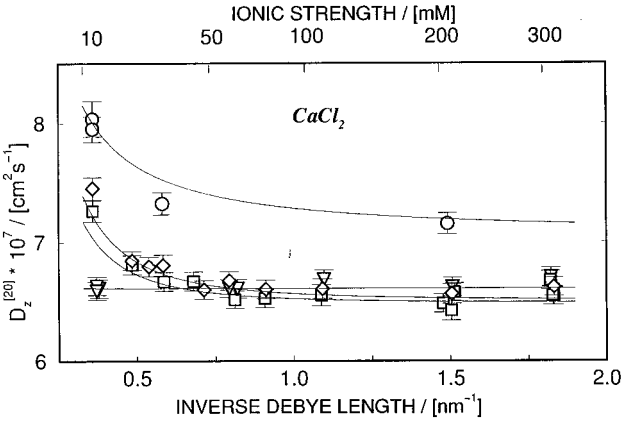

Figure 2. Experimental diffusion coefficient $D_z^{[20]}$ vs the inverse of Debye screening length (or ionic strength) measured at a hemoglobin concentration $c = 5$ mg/mL. The ionic strength ($10 \leq I_s \leq 300$ mM) is due to $CaCl_2$ added to the proper buffer at $I_s \simeq 10$ mM for pH = 5.4 (○), 7.2 (▽) 9.1 (□), and 9.4 (◇). Solid lines have the same meaning as in Figure 1.

Measurements with NaCl. The hemoglobin diffusion coefficients $D_z^{[20]}$ at increasing ionic strength ($10 \leq I_s \leq 300$ mM) due to added NaCl are reported in Figure 1 vs the inverse of Debye screening length (see eq 8) for pH = 7.3 in Phosphate buffer and for pH = 9.3 in borate buffer. In the same Figure also reported are previous data[14] relative to acid conditions (pH = 5) in the same range of ionic strength (acetate buffer + NaCl) investigated here.

Measurements with $CaCl_2$. The diffusion coefficients $D_z^{[20]}$ shown vs the inverse of Debye screening length in Figure 2 are obtained from Hemoglobin solutions at increasing ionic strength ($10 \leq I_s \leq 300$ mM) due to added $CaCl_2$. The data refer to conditions of pH = 7.2 in phosphate or Tris buffers, of pH = 9.1 and pH = 9.5 in borate buffer and pH = 5.4 in acetate buffer.

The protein diffusion coefficient $D_z^{[20]}$ decreases vs ionic strength both at alkaline and acid conditions but is almost constant for neutral pH. It is worth noting that, at $I_s \simeq 50-80$ mM, $D_z^{[20]}$ reaches different saturation values, for the acid and alkaline conditions. Similar differences are found between the data taken at similar values of pH and different types of salt, NaCl or $CaCl_2$. This seems to indicate that the changes are not functions of ionic strength alone but are salt specific; i.e., they could result from specific adsorption of ions onto protein surface. However, at present, the interpretation of this point is somewhat qualitative and further measurements, at different protein concentrations' with different electrolytes, could help. We must add also that satisfactory models do not seem available.

As a check of the role of different ions, measurements have also been performed in the absence of Cl^- by varying the ionic strength with Borate $Na_2B_4O_7$. The behavior of the diffusion coefficient vs ionic strength is very similar to that of other measurements at alkaline condition ($D_z^{[20]}$ data not shown).

5. Discussion

The data reported in this paper (see Figures 1 and 2) show that the hemoglobin diffusion coefficient $D_z^{[20]}$ depends on pH and ionic strength or equivalently the inverse of Debye screening length (see eq 8). The following discussion is aimed at the elucidation of the effects of ionic strength upon the measured diffusional properties, by considering also intermolecular interactions effects due to finite, although low, protein concentration.[8]

As a matter of fact, since hemoglobin is known to dissociate from tetramers to dimers, both bearing significant electrostatic charges ($-15 \leq Q_T \leq +15$) away from the isoelectric point, the changes in the mutual diffusion coefficient can be understood in terms of both intermolecular interactions and dissociation.[8] In this respect the protein solution is modeled as a multicomponent system of interacting species. The dissociation is assumed to lead to a bimodal distribution of masses corresponding to tetramers $\alpha^2\beta^2$ and dimers $\alpha\beta$: each species interacting with the others: i.e., tetramers−tetramers, dimers−dimers, and tetramers−dimers. The interaction occurs through the screened electrostatic, the hard core, and, perhaps, a short range attractive potential. At low ionic strength ($I_s \leq 100$ mM), the main component of the potential energy, with the exception of the protein at the isoelectric point, is the screened Coulomb potential while the short range attractive potential becomes relevant ad high I_s. Since most of the $D_z^{[20]}$ changes occur at $I_s \leq 100$ mM, the following preliminary discussion of the data accounts for the electrostatic potential alone.

Actually the electrolytes influence the strength of protein electrostatic interactions mainly by modulating the protein−protein repulsion through the screening of their charges and this effect appears as the increase of $D_z^{[20]}$ when lowering the ionic strength (see eq 10). Changes in the screening of the electrostatic potential energy induce perturbations also on the intersubunits interactions that lead to protein dissociation into dimers. The ionic strength dependence of dissociation and its effect on PCS measurements has been modeled by Lunelli et al. by taking into account the electrostatic interactions according to the Debye−Hückel theory as suggested by Tanford.[11,13,14] This model is refined here in order to introduce the effect of the intermolecular interactions on the measured $D_z^{[20]}$.

If we assume that we can ideally switch on or off either charge effect, we can then assess the contribution of the individual phenomena to the observed trend of $D_z^{[20]}$. In this way, at first, we can try to interpret the

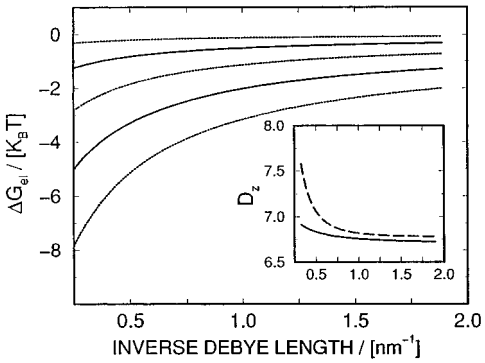

Figure 3. Electrostatic dissociation free energy ΔG_{el} vs the inverse of Debye screening length, evaluated according to $\Delta G_{el}(I_s = 0.3\ M) + \Delta G_{nel} = -ln(1)$. The protein charge Q_T is 4, 8, 12, 16, and 20 from top to bottom. The inset shows the behavior of the diffusion coefficient D_z vs the inverse Debye screening length according to the pure dissociation case (model B) (solid line) and the pure interaction case (model C) (dashed line) with $Q_T = 12$.

change in $D_z^{[20]}$ as resulting entirely from changes in molecular weight, i.e, as due to protein dissociation in a system free of interparticles interactions. This trend is evaluated according to eq 10 with $\tilde{k} = 0$. The thermodynamics of Hemoglobin dissociation is described by the free energy ΔG_{diss}, assumed to be the sum (see eq 5) of an electrostatic contribution, ΔG_{el}, following the Tanford model previously described,[11] and of a term ΔG_{nel} independent of the electrostatic interactions, which can be taken as an additional quantity to be determined. If ΔG_{el} is computed according to the Tanford model (eqs 4 and 7), an increase in $D_z^{[20]}$ is observed when lowering I_s. If one takes as a reference condition, $\Delta G_{diss} = \Delta G_{el}(I_s = 0.3\ M) + \Delta G_{nel} = 0$, corresponding to $L_{diss} = 1$, a behavior of ΔG_{el} vs I_s is found as shown in Figure 3. When the protein charge is relevant, e.g. $|Q| \geq 10$, then ΔG_{diss} has a remarkable dependence on the ionic strength and $D_z^{[20]}$ decreases from the dimer's value to the tetramer's value (see inset of Figure 3 where $Q_T = 12$), therefore indicating an enhanced association of dimers into tetramers.

On the other hand the dependence of $D_z^{[20]}$ upon ionic strength can be viewed as due to the effect of interparticle interactions alone in a system at a fixed fractions of dimers, in which any dependence of dissociation upon ionic strength has been neglected: i.e., $\Delta G_{el} = 0$. For the sake of comparison with the previous case, let us assume hemoglobin bearing $Q_T = 12$ with $\Delta G_{diss} = -\ln(L_{diss} = 1) = \Delta G_{nel}$ (corresponding to pH ≃ 9.5). The introduction of the intermolecular interactions, i.e. $\tilde{k} \neq 0$ (eq 10), substantially raises the diffusion coefficient in the whole I_s range and enhances the increase of D_z at low I_s (see inset of Figure 3).

Then, both interactions and electrostatic driven dissociation lead to rising D_z when lowering I_s, as actually observed (Figures 1 and 2). However, from the previous discussion it is not clear whether to account for the experimental trend of D_z on the basis either of interactions or dissociation. One could obtain an acceptable fit of the experimental data from interparticle interactions only or from protein dissociation alone, but, obviously, it appears more reasonable to proceed by means of a model which takes into account both phenomena.

Three cases are then considered and compared: model A (A = B + C), which takes into account intermolecular interactions and electrostatic contributions to ΔG_{diss}, i.e., $\Delta G_{el} \neq 0$ and $\tilde{k} \neq 0$; model B, where no intermolecular interactions are present, i.e., $\tilde{k} = 0$ in eq 10, and $\Delta G_{el} \neq 0$; model C where $\tilde{k} \neq 0$ and $\Delta G_{el} = 0$, i.e, ΔG_{diss} independent of ionic strength I_s. Since $D_z^{[20]}$ displays appreciable changes at low ionic strengths and a reduced number of fitting parameters is always to be preferred, the attractive potential is, to a first approximation, disregarded by keeping $H = 0$.

Table 1. Best Fit Parameters of the Single Data Sets[a]

	model A = B + C $\Delta G_{el} \neq 0$; $k \neq 0$			model B $\Delta G_{el} \neq 0$; $\tilde{k} = 0$			model C $\Delta G_{el} = 0$; $\tilde{k} \neq 0$		
pH	D_T^o	ΔG_{nel}	$\|Q_T\|$	D_T^o	ΔG_{nel}	$\|Q_T\|$	D_T^o	ΔG_{nel}	$\|Q_T\|$
				NaCl					
5.0[b]	5.85	−4.06	11.74	6.72	2.3	19	6.82	0.001	10.5
7.3	6.50	0.59	0.05	6.65	−1.90	0.0	6.56	0.1	0.02
9.3	6.66	4.52	12.0	6.69	5.05	23.3	6.68	0.01	12.2
				$CaCl_2$					
5.4	7.04	17.2	13.4	7.13	8.5	27.7	6.79	2.7	14.5
7.2	6.32	−1.2	0.07	6.63	−1.9	0.0	6.47	0.5	0.04
9.1	6.45	13.9	12.2	6.52	9.8	29.1	5.8	34	14.9
9.4	6.47	12.7	13.8	6.58	10.9	30.6	5.96	16.6	16.1
				Borate Buffer					
9.5	6.60	14.4	13	6.68	8.5	27.6	5.86	49.4	16.1

[a] Hemoglobin diffusion coefficient D_T^o (in 10^{-7} cm^2s units), nonelectrostatic free energy ΔG_{nel} contribution (in K_BT units) and charge Q_T (in esu) obtained by fitting the single set of data with the three models described in the text. χ^2 was always ≤ 1. [b] Data from Lunelli et al. (1994).

Fits of the data sets corresponding to different salts and pH values have been performed separately in order to discriminate among the three cases: details on the fitting procedures are given in the Experimental Section. The free parameters are then: the tetramer single particle diffusion coefficient D_T^o, the absolute value of the tetramer charge Q_T, and the dissociation free energy ΔG_{diss}.

The best fit parameters, all corresponding to $\chi^2 \leq 1$, are summarized in Table 1, for the NaCl, $CaCl_2$, and borate buffer solutions and for pH values in the range $5 \leq pH \leq 9.5$. The single particle diffusion coefficients D_T^o obtained by a fit with the complete model A and the pure dissociation model B are $D_T^o = (6.48 \pm 0.3) \times 10^7$ cm^2/s and $D_T^o = (6.7 \pm 0.2) \times 10^7$ cm^2/s both in reasonable agreement with previous results at low ionic strength[8] (i.e. $D_T^o = (6.58 \pm 0.06) \times 10^7$ cm^2/s), while that obtained from the pure interaction model C, $D_T^o = (6.36 \pm 0.4) \times 10^7$ cm^2/s, is slightly lower. This last result makes one feel that model C is not particularly suitable to describe diffusion vs electrolyte screening.

The tetramer charge Q_T is vanishing for all the three models at pH ≃ 7: this value is the known hemoglobin isoelectric pH above which $Q_T \leq 0$. However the slope of Q_T is different for the three models (see Figure 4). In particular, the value predicted by model B is higher than that usually found for hemoglobin[11,14,31−33] and this suggests that the pure dissociation model B does not yield a consistent picture of the protein behavior in solution, though apparently describing the experimental data. Finally, the complete model A seems both to accurately fit the data and to give reasonable values of D_T^o and Q_T and therefore in the following only this model will be considered. This model was found to describe the trend of D_z vs protein concentration at fixed I_s, although a comparison with model C was not possible since the ionic strength was not varied.[8]

As to the parameter ΔG_{nel}, the relevant variation found for the best fit values indicates a probable

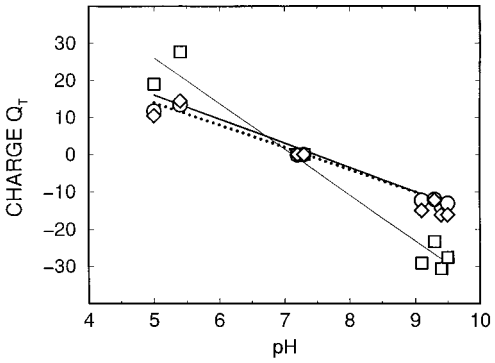

Figure 4. Hemoglobin charge Q_T vs solution pH obtained from data fitting with the three cases discussed in the text: model A (○); model B (□); model C (◇). The thin solid line is the linear regression with Model B. Thick solid and dotted lines are the global fit result for $H = 4.5$ and $H = 0$ (see Table 2), respectively.

Table 2. Global Analysis with Best Fit Parameters of the Data[a]

D_T^o	q_i	q_s	pH_{iso}	H
Global Analysis				
6.44 ± 0.1	44 ± 7	-6.0 ± 0.8	7.25 ± 0.18	0*
6.58*	48.6 ± 7	-6.5 ± 0.8	7.4 ± 1.4	4.53 ± 0.8
Single Fit Summary				
6.5 ± 0.3	44.2 ± 2	-6.1 ± 0.3	7.24 ± 0.18	0*

[a] Hemoglobin diffusion coefficient D_T^o (in 10^{-7} cm^2/s units), charge $Q_T = q_i + pH \times q_s$, (in esu) and $pH_{iso} = -q_p/q_i$, Hamaker constant H (in K_BT units), obtained from global analysis of the data with model A described in the text. The single fit summary is obtained from Table 1 (model A). The values marked with an asterisk are kept fixed during the fit.

overfitting of the data that suggests dropping the additional parameter, the Hamaker constant, in the fitting. In order to avoid such problems and to obtain more accurate estimates for the parameters, an increase of the number of data points to be fitted simultaneously to the theoretical model was desirable and a global analysis of the data, collected at different pH and I_s, was performed.

The global analysis is made possible by reasonably assuming D_T^o, the single particle diffusion coefficient of the tetrameric hemoglobin, to be the same at all pH values in the observed range and the protein charge to be fairly well described by a linear law vs pH, $Q_T = q_i + (pH)\, q_s$.[11] Furthermore a single value of the Hamaker constant was assumed and pH dependent values of the ΔG_{nel} free energy have been used. All together a fit of 56 experimental points was performed with 11 parameters, and the result is summarized in Table 2. In a first global analysis H is kept fixed at $H = 0$ and D_T^o is let as a free parameter of the fit. In the second case, D_T^o is kept fixed at $D_T^o = 6.58 \times 10^7$ cm^2/s, previously found,[8] and the Hamaker constant H is a free parameter of the fit. In both cases the global analysis can be successfully performed ($\chi^2 \simeq 1$) and the best fit curves, with $H = 4.5$ (see Table 2), are shown in Figures 1 and 2.

The trend of the protein charge vs pH is found to be in agreement with what expected and found by the single-set fits with model A. The results are summarized for comparison to the global fit in Table 2 (see Figure 4).

The single particle diffusion coefficient $D_T^o = (6.44 \pm 0.1 \times 10^7$ cm^2/s is found slightly lower than the reference value $D_T^o = 6.58 \times 10^7$ cm^2/s, when the short range attractive potential is neglected ($H = 0$). On the other hand, when D_T^o is kept at 6.58×10^7 cm^2/s, reasonable values (of order of K_BT)[7] of the Hamaker constant ($H = 4.5$) are found, while, as a check, by keeping D_T^o at 6.44×10^7 cm^2/s a value of H very close to zero is found.

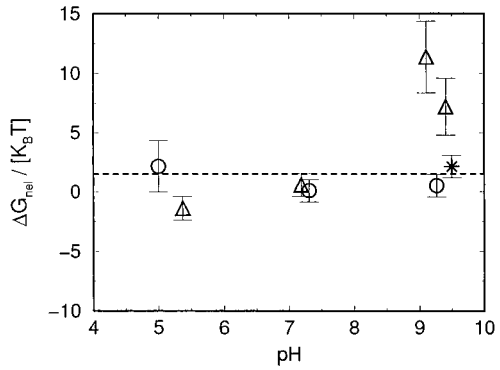

Figure 5. Nonelectrostatic contribution ΔG_{nel} to the free energy of dissociation vs solution pH obtained by global analysis ($H = 4.5$). The different symbols refer to NaCl (□) and $CaCl_2$ (△) salts and borate buffer (*). The horizontal dashed line corresponds to the best fit value obtained when the global analysis is performed by fitting ΔG_{nel} as a single value for all the data.

The best fit values of ΔG_{nel} obtained from global analysis, which includes the short range attractive potential, have been plotted vs pH in Figure 5. In the case of monovalent added electrolyte (NaCl), a small contribution to the total free energy is evident; i.e., $\Delta G_{nel} = 0.5(\pm 1)K_BT$. When the divalent electrolyte, $CaCl_2$, is used then, a slight dependence upon pH of ΔG_{nel} is observed which, however, seems to be weakened by the comparable experimental uncertainties: $\Delta G_{nel}(pH \simeq 5) \simeq -2.5 \pm 2K_BT$ and $\Delta G_{nel}(pH \simeq 9) \simeq 8 \pm 5K_BT$. As a matter of fact, when the global analysis is performed by fitting ΔG_{nel} as a single value common to all pH, one finds almost the same fit values as before for Q_T, H, and D_T^o, and the nonelectrostatic contribution is found to be $\Delta G_{nel} = (1.5 \pm 1)K_BT$. This estimate is related to the asymptotic values of $D_z^{[20]}$ at high ionic strengths and corresponds to a residual protein dissociation $x \simeq 20\%$.

In conclusion, the different roles of electrostatic protein charge, counterion screening and dissociation on the mutual diffusion coefficient $D_z^{[20]}$ of hemoglobin solutions have been described. Though either intermolecular interactions or intersubunits dissociation could lead to an apparently satisfactory description of the experimental trend of $D_z^{[20]}$, it is shown here that a more consistent picture of the hemoglobin diffusion, in solutions at different ionic strengths and pH, requires the presence of both interactions and dissociation, the latter established by previous investigations, even at volume fractions as low as $\phi = 0.005$. A global analysis of the data collected at different values of pH, salt types, and ionic strength allows the estimate of the protein charge and the electrostatic and the nonelectrostatic component to the free energy of dissociation of tetramers into dimers. The results suggest that a more detailed picture of protein behavior is achieved by performing accurate measurements and by employing realistic models of colloid physics, with a consequent better understanding of equilibria and aggregation phenomena ubiquitous in protein solutions.

Acknowledgment. The authors are grateful to Enrico Bucci for kindly providing hemoglobin stock

samples and for enlightening suggestions.

References and Notes

(1) George, A.; Wilson, W. W. *Acta Crystallogr., D* **1995**, *50*, 361.
(2) Naegele, G. *Phys. Rep.* **1996**, *272*, 215−372.
(3) Pecora, R., Ed.; *Dynamic Light Scattering*; Plenum Press: New York, 1985.
(4) Brown, W., Ed.; *Dynamic Light Scattering, The method and some applications*; Clarendon Press: Oxford, 2nd ed.; 1993.
(5) Chu, B. *Laser Light Scattering*, Academic Press, Inc.: San Diego, CA, 1991.
(6) Berne, B. J.; Pecora, R. *Dynamic Light Scattering*; J. Wiley and Sons, Inc: New York, 1976.
(7) Muschol, M.; Rosenberger, F. *J. Chem. Phys.* **1995**, *103*, 10424−10432.
(8) Beretta, S.; Chirico, G.; Arosio, D.; Baldini, G. *J. Chem. Phys.* **1997**, *106*, 8427−8435.
(9) Antonini, E.; Brunori, M. *Hemoglobin and Myoglobin in their Reaction with Ligands*; North-Holland Publishing Company: Amsterdam, 1971.
(10) Gryczynski, Z.; Beretta, S.; Lubkowski, J.; Razynska, A.; Gryczynski, I.; Bucci, E. *Biophys. Chem.* **1997**, *64*, 81−91.
(11) Lunelli, L.; Bucci, E.; Baldini, G. *Phys. Rev. Lett.* **1993**, *70*, 513−516.
(12) Stigter, D. *Biophys. J.* **1995**, *69*, 380−388.
(13) Tanford, C. *Physical chemistry of macromolecules*, 2nd ed.; John Wiley and Sons: New York, 1963.
(14) Lunelli, L.; Zuliani, P.; Baldini, G. *Biopolymers* **1994**, *34*, 747−757.
(15) Berjiis, M.; Sharma, V. S. *Anal. Biochem.* **1991**, *196*, 223−228.
(16) Pusey, P. N.; Tough, R. J. A. Particle Interactions. In *Dynamic Light Scattering*; Pecora, R., Ed.; Plenum Press: New York, 1985.
(17) Corti, M.; Degiorgio, V. *J. Phys. Chem.* **1981**, *85*, 711−717.
(18) Felderhof, B. U. *J. Phys. A: Math. Gen.* **1978**, *11*, 929−937.
(19) Ohshima, H.; Mishonova, E.; Alexov, E. *Biophys. Chem.* **1996**, *57*, 189−203.
(20) Petsev, D. M.; Denkov, N. D.; Nagayama, K. *Chem. Phys.* **1993**, *175*, 265−270.
(21) Belloni, L.; Drifford, M. *J. Phys. Lett.* **1985**, *46*, L1183.
(22) Bucci, E.; Malak, H.; C. Fronticelli,; Gryczynski, I.; Lakowicz, J. *J. Biol. Chem.* **1988**, *263*, 6972−6977.
(23) Assendelft, O. W. V.; Zijlstra, W. G. *Anal. Chem.* **1975**, *69*, 43.
(24) Koppel, D. E. *J. Chem. Phys.* **1972**, *57*, 4814−4820.
(25) Beretta, S.; Lunelli, L.; Chirico, G.; Baldini, G. *Appl. Opt.* **1996**, *35*, 3763−3770.
(26) Weast, R. C.; Astle, M. J. *CRC Handbook of Chemistry and Physics*; 63rd ed.; CRC Press: Boca Raton, FL, 1982−1983.
(27) Hall, R. S.; Oh, Y. S.; Johnson, C. S., Jr. *J. Phys. Chem.* **1980**, *84*, 756−767.
(28) Sanders, A. H.; Cannell, D. S. In *Light Scattering in liquids and macromolecular solutions*; Degiorgio, V., Corti, M., Giglio, M., Eds.; Plenum Press: New York, 1980.
(29) Bevington, P. R. *Data Reduction and Error Analysis for the Physical Sciences*; McGraw-Hill Inc.: New York, 1969.
(30) Press, W. H.; Teukolsky, S. A.; Vetterling, W. T.; Flannery, B. P. *Numerical Recipes in C. The art of scientific computing*; Cambridge University Press: New York, 1992.
(31) Haas, D. D.; Ware, B. R. *Biochemistry* **1978**, *17*, 4946−4950.
(32) Rollema, H. S.; Bruin, S. H. D.; Janssen, L. H. M.; Os, G. A. J. *J. Biol. Chem.* **1975**, *250*, 1333−1339.
(33) Bucci, E.; Fronticelli, C.; Ragatz, B. *J. Biol. Chem.* **1968**, *243*, 241−249.

MA971137L